U.S. DEPARTMENT OF ENERGY

PNNL-18363

Prepared for the
U.S. Nuclear Regulatory Commission
under a Government Order
with the U.S. Department of Energy
Contract DE-AC05-76RL01830

Task 1 Final Report

Theoretical/Mathematical Modeling of Ultrasonic Wave Propagation in Anisotropic Polycrystalline Stainless Steels

S. Ahmed
M. T. Anderson

April 2009

Pacific Northwest
NATIONAL LABORATORY

DISCLAIMER

PACIFIC NORTHWEST NATIONAL LABORATORY
operated by
BATTELLE
for the
UNITED STATES DEPARTMENT OF ENERGY
under Contract DE-AC05-76RL01830

Printed in the United States of America

Available to DOE and DOE contractors from the
Office of Scientific and Technical Information,
P.O. Box 62, Oak Ridge, TN 37831-0062;
ph: (865) 576-8401
fax: (865) 576-5728
email: reports@adonis.osti.gov

Available to the public from the National Technical Information Service,
U.S. Department of Commerce, 5285 Port Royal Rd., Springfield, VA 22161
ph: (800) 553-6847
fax: (703) 605-6900
email: orders@ntis.fedworld.gov
online ordering: http://www.ntis.gov/ordering.htm

This document was printed on recycled paper.
(9/2003)

PNNL-18363

Task 1 Final Report

Theoretical/Mathematical Modeling of Ultrasonic Wave Propagation in Anisotropic Polycrystalline Stainless Steels

S. Ahmed[(a)]
M. T. Anderson

April 2009

Prepared for
U.S. Nuclear Regulatory Commission
under a Government Order
with the U.S. Department of Energy
Contract DE-AC05-76RL01830

Pacific Northwest National Laboratory
Richland, Washington 99352

(a) Sonsight, Inc., Accokeek, Maryland 20607

Summary

One of the tasks of the U.S. Nuclear Regulatory Commission-sponsored project titled "Reliability of Nondestructive Examination (NDE) for Nuclear Power Plant (NPP) Inservice Examination (ISI)" is to provide collaborative assistance to Commissariat à l'Energie Atomique (CEA) in France through theoretical predictions of ultrasonic scattering by grains of cast stainless steels (CASS) components. More specifically, a mathematical treatment of ultrasonic scattering in media having duplex micro-structure is sought because cast stainless steel components often contains larger-scale macrograins that are composed of sub-grains/colonies.

In this report, we present formal mathematical theories for ultrasonic wave propagation in polycrystalline aggregates having both simple (composed of grains only) and complex microstructures (having macrograins and sub-grains/colonies). Computations based on these theories are then carried out for ultrasonic backscatter power, attenuation due to scattering, and phase velocity dispersions. Specifically, numerical results are presented for the backscatter coefficient for a plane longitudinal wave propagating in duplex steel containing macrograins and colonies. Furthermore, the expected propagation characteristics (attenuation coefficient and phase velocity) are computed and described in this report for plane longitudinal waves propagating in (1) steels composed of randomly oriented grains, (2) [001] aligned grains encountered in austenitic stainless steel welds and castings, and (3) duplex steels. Our analysis shows that both backscatter and attenuation are dominated by scattering from macrograin boundaries for the low non-dimensional frequency, ka_m. Colonies do not cause noticeable additional backscatter and attenuation for $ka_m \leq 2$ in the case of equiaxed macrograins and colonies. This threshold frequency at which contributions from colonies is visible is reduced ($ka_m \approx 1$) for elongated macrograins and colonies.

Acronyms and Abbreviations

CASS	cast stainless steels
CEA	Commissariat à l'Energie Atomique
ISI	inservice inspection
NDE	nondestructive examination
NPP	nuclear power plant

Contents

Figures

Tables

1.0 Theory of Ultrasonic Backscattering from Duplex Microstructures

Many metallic alloys exhibit internal structure on several length scales. On the smallest scale are individual micrograins; that is, single crystals of metal with atoms arranged in a regular lattice. Neighboring micrograins with aligned or partially aligned lattices can form larger entities, such as platelets, colonies, or macrograins. The largest structures, macrograins, are often visible without magnification when polished metal surfaces are properly etched.

Electrical signals received by an ultrasonic NDT system from defects occupying region V_F generated by time-harmonic acoustic waves of angular frequency ω can be modeled using the Thompson-Gray measurement model (1993) as follows.Equation Section 1

$$\delta\Gamma = \frac{1}{4P}\int_{V_F} i\omega(\omega^2\delta\rho u_i^o u_i - \delta c_{ijkl}u_{i,j}^o u_{k,l})\,d\Omega\,. \tag{1.1}$$

Here, P represents the electrical power propagating the cables, superscript "o" represents field variables without defects, $\delta\rho$ denotes the density difference between a host medium and defect, and δc_{ijkl} refers to similar differences in elastic constants. If scatterer density fluctuations can be neglected, then

$$\delta\Gamma = -\frac{i\omega}{4P}\int_{V_F} \delta c_{ijkl}u_{i,j}^o u_{k,l}\,d\Omega \tag{1.2}$$

Using Rose's notation (Rose 1992), we observe that

$$\delta\Gamma = \frac{1}{\left(4\pi\rho v_l^2\right)}\int_{V_F} \delta c_{ijkl}u_{i,j}^o u_{k,l}\,d\Omega \tag{1.3}$$

Invoking weak scattering (Born) approximation, that is, $u_i = u_i^o$, and considering plane waves of the form $u_i^o = U_o\hat{u}_i e^{-i\vec{k}\bullet\vec{r}}$ ($\hat{u}_i$, U_o, $\vec{r}$, and $\vec{k} = \hat{k}k$ representing particle polarization, amplitude, position vector, and propagation vector, respectively)

$$\delta\Gamma = \frac{k^2\hat{k}_j\hat{k}_l\hat{u}_i\hat{u}_k U_o^2}{\left(4\pi\rho v_l^2\right)}\int_{V_F} \delta c_{ijkl}e^{-2i\vec{k}\bullet\vec{r}}\,d^3\vec{r} \tag{1.4}$$

where $d\Omega = d^3\vec{r}$ is a differential volume at $\vec{r}$.

Hence, the expected (denoted by $\langle..\rangle$) scattered ultrasonic power at the receiver is

$$\left\langle \delta\Gamma\delta\Gamma^{*}\right\rangle = \left\langle \frac{k^4 U_o^4 \hat{k}_j \hat{k}_l \hat{k}_n \hat{k}_q \hat{u}_i \hat{u}_k \hat{u}_m \hat{u}_p}{\left(4\pi\rho v_l^2\right)^2} \int d^3\vec{r} \int_{V_F} \delta c_{ijkl}(\vec{r})\delta c_{mnpq}(\vec{r}')e^{-2i\vec{k}\bullet(\vec{r}-\vec{r}')}\, d^3\vec{r}' \right\rangle \tag{1.5}$$

The evaluation of the integral is simplified by the following coordinate transformation $\vec{p} = \frac{\vec{r}+\vec{r}'}{2}$, $\vec{s} = \vec{r} - \vec{r}'$ yielding together with the assumption of statistical homogeneity

$$\left\langle \delta\Gamma\delta\Gamma^{*}\right\rangle = \frac{k^4 U_o^4 \hat{k}_j \hat{k}_l \hat{k}_n \hat{k}_q \hat{u}_i \hat{u}_k \hat{u}_m \hat{u}_p}{\left(4\pi\rho v_l^2\right)^2} \int_{V_F} d^3\vec{s} \int_{V_F} \left\langle \delta c_{ijkl}(\vec{p}+\vec{s}/2)\delta c_{mnpq}(\vec{p}-\vec{s}/2)\right\rangle e^{-2i\vec{k}\bullet\vec{s}}\, d^3\vec{p} \tag{1.6}$$

For a statistically homogeneous medium, we can write

$$\left\langle \delta c_{ijkl}(\vec{p}+\vec{s}/2)\delta c_{ijkl}(\vec{p}-\vec{s}/2)\right\rangle = P^M(\vec{s})\left\langle \delta c^M_{ijkl}(\gamma)\delta c^M_{mnpq}(\gamma)\right\rangle_{\Xi}. \tag{1.7}$$

Here $P^M(\vec{s})$ is the probability that the line segment $\vec{s}$ lies in the same macrograin and γ is the Euler angle of the macrograin with the subscript Ξ referring to the set of possible Euler angles.

Rose (1992) has shown that the foregoing equation is equivalent to

$$\left\langle \delta\Gamma\delta\Gamma^{*}\right\rangle = \frac{k^4 U_o^4 \hat{k}_j \hat{k}_l \hat{k}_n \hat{k}_q \hat{u}_i \hat{u}_k \hat{u}_m \hat{u}_p}{\left(4\pi\rho v_l^2\right)^2} \Omega \left\langle \delta c^M_{ijkl}(\gamma)\delta c^M_{mnpq}(\gamma)\right\rangle_{\Xi} \int_{V_F} P^M(\vec{s}) e^{-2i\vec{k}\bullet\vec{s}}\, d^3\vec{s} \tag{1.8}$$

where $\Omega = \frac{\left\langle v_g^2 \right\rangle}{\left\langle v_g \right\rangle} N$ with v_g representing the volume of one macrograin out of *N* different macrograins affected by a given ultrasonic beam and $\langle .. \rangle$ representing ensemble averages.

Therefore, the backscattered power generated by an ultrasonic beam propagating in the 3-direction is given by

$$\left\langle \delta\Gamma\delta\Gamma^{*}\right\rangle = \frac{k^4 U_o^4}{\left(4\pi\rho v_l^2\right)^2} \Omega \left\langle \delta c^M_{3333}(\gamma)\delta c^M_{3333}(\gamma)\right\rangle_{\Xi} \int_{V_F} P^M(\vec{s}) e^{-2i\vec{k}\bullet\vec{s}}\, d^3\vec{s} \tag{1.9}$$

One can define the following backscatter coefficient, which depends only on the material microstructure.

$$\eta = \frac{k^4}{\left(4\pi\rho v_l^2\right)^2} \left\langle \delta c^M_{3333}(\gamma)\delta c^M_{3333}(\gamma)\right\rangle_{\Xi} \int_{V_F} P^M(\vec{s}) e^{-2i\vec{k}\bullet\vec{s}}\, d^3\vec{s}\,. \tag{1.10}$$

Difficulties in predicting backscattering coefficient η for multiphase materials with complex microstructures having different length scales (macrograins, colonies, and micrograins) arise through the evaluation of the two-point correlation function $\left\langle \delta c^{M}_{3333}(\gamma)\delta c^{M}_{3333}(\gamma)\right\rangle_{\Xi}$, especially when there exists crystallographic orientation relationships between macrograins and colonies.

Utilizing the arguments presented by Han and Thompson (1997), the two-point correlation function is written as

$$\left\langle \delta c^{M}_{3333}(\gamma)\delta c^{M}_{3333}(\gamma)\right\rangle_{\Xi} = \left\langle \delta c^{P}_{3333}\delta c^{P}_{3333}\right\rangle PP(\vec{s}) + \sum_{P\neq Q}\left\langle \delta c^{P}_{3333}\delta c^{Q}_{3333}\right\rangle PQ(\vec{s}) \tag{1.11}$$

where P and Q are colony indices. The first term represents the case when two points separated by $\vec{s}$ are in an elastically equivalent variant, which occurs with probability $PP(\vec{s})$. The second term addresses the case when the two points in question are an elastically distinct variant, which occurs with probability $PQ(\vec{s})$. For large $|\vec{s}|$, $PQ(\vec{s})$ would approach zero in the case of macrograins with random orientation. However, if only $N_{distinct}$ variants are allowed, it would have a limiting value of $1/N_{distinct}$.

1.1 Special Cases for Calculations

For equiaxed macrograins/colonies, we have employed the following geometric autocorrelation function (Stanke and Kino 1984).

$$P^{M/C}(\vec{s}) = e^{-|\vec{s}|/a}. \tag{1.12}$$

Generalizing on this, the geometric autocorrelation function $W(\vec{s})$ for elongated (spheroid) macrograins (Ahmed and Thompson 1991) is taken to have the form (schematic shown in Figure 1.1).

$$P^{M/C}(\vec{s}) = e^{-|\vec{s}|\sqrt{1+(a^2/c^2-1)\cos^2(\theta))}/a}. \tag{1.13}$$

In the aforementioned equations, a represents the semi-axis perpendicular to the incident wave, c represents the semi-axis parallel to the incident wave, and θ is the angle that the position vector $\vec{s}$ makes with respect to the propagation direction of the incident ultrasonic wave.

1.1.1 Results for Duplex Stainless Steel

In this report, we show numerical predictions for backscatter coefficients for a complex microstructure possessed by duplex stainless steel. In our calculations, the crystallographic orientation relationship between austenite (fcc) and ferrite (bcc), described by the well-known Kurdjumov-Sachs (K-S) description (Kurdjumov and Sachs 1930), $\{111\}_{fcc} \parallel \{1\,\bar{1}\,0\}_{bcc}$ and $<1\,\bar{1}\,0>_{fcc} \parallel <111>_{bcc}$, is assumed to describe the crystallographic relationship between a macrograin and the associated colony. It is also assumed that there are only two elastically distinct variants of colonies (i.e., $N_{distinct} = 2$). The two-point averages required in Eq. (1.10) are computed from Eq. (1.11). The same description of the orientation relationship between macrograin and colony will also be utilized later when expected propagation constants of plane longitudinal elastic waves in duplex steel are computed.

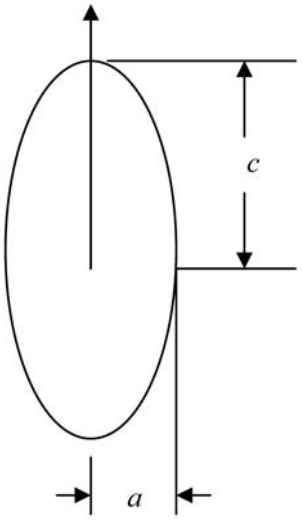

Figure 1.1. Schematic Representation of Macrograin/Colony

The fluctuations in elastic constants are measured related to unweighted Voigt (1928) averaged elastic constant; that is, $\delta c_{ijkl} = c_{ijkl}(\vec{r}) - c^{o}_{ijkl}$. The single crystal elastic constants and material density employed in the calculations are listed in Table 1.1 (Kupperman and Reimann 1978).

Table 1.1. Austenitic Elastic Constants and Reported Density

Single Crystal Elastic Constants			**Polycrystalline Stainless Steel Density**
$c_{11}\left(\times 10^{12}\,\frac{dynes}{cm}\right)$	$c_{12}\left(\times 10^{12}\,\frac{dynes}{cm}\right)$	$c_{44}\left(\times 10^{12}\,\frac{dynes}{cm}\right)$	$\rho\,\frac{gm}{cm^3}$
0.216	0.145	0.129	7.86

Before proceeding with the presentation of numerical results, it is worthwhile to point out that the presence of two scales in the microstructure contributes to the scattering process by two mechanisms. First, preferential orientation of colonies associated with a macrograin influences the two-point correlation functions significantly. Second, colonies themselves act as secondary scatterers of ultrasonic waves.

Figure 1.2 shows absolute backscatter coefficients for an incident ultrasonic wave propagating in the 3-direction of the laboratory (sample) coordinate system when both macrograins and colonies are equiaxed. Our numerical predictions suggest that with the presence of very small colonies (diameter ratio of up to 0.001), there is no appreciable effect of their presence for non-dimensional frequencies $ka_m \le 2$ when the macrograins/colonies are equiaxed. It should be noted here that for the idealized duplex microstructure chosen in this calculation, $ka_m = 2$ refers to a frequency of 6.06 MHz for a transverse macrograin diameter of 1 mm.

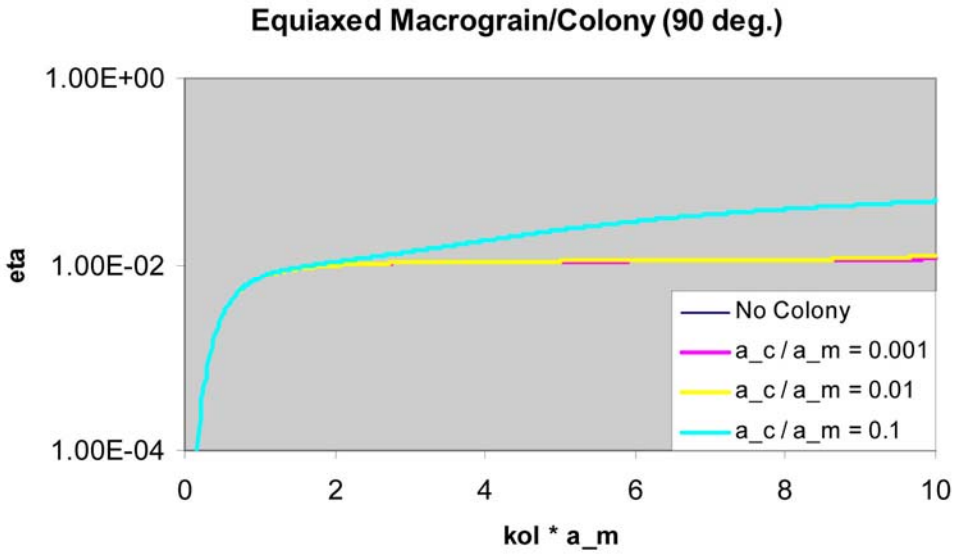

Figure 1.2. Normalized and Absolute Backscatter Coefficients for Ultrasonic Wave Propagating in the 3-Direction of the Sample Coordinate System for Equiaxed Macrograins and Colonies

Next we consider both macrograins and colonies to have spheroidal shapes. Figure 1.3 describes the results in this case for a macrograin aspect ratio (c_m / a_m) of 2.0. We assumed the colonies to have the same aspect ratio. For elongated macrograins/colonies, additional colony contributions to the backscatter become noticeable for $ka_m \approx 1.0$. This corresponds to a frequency of approximately 3 MHz for a macrograin transverse diameter of 1 mm.

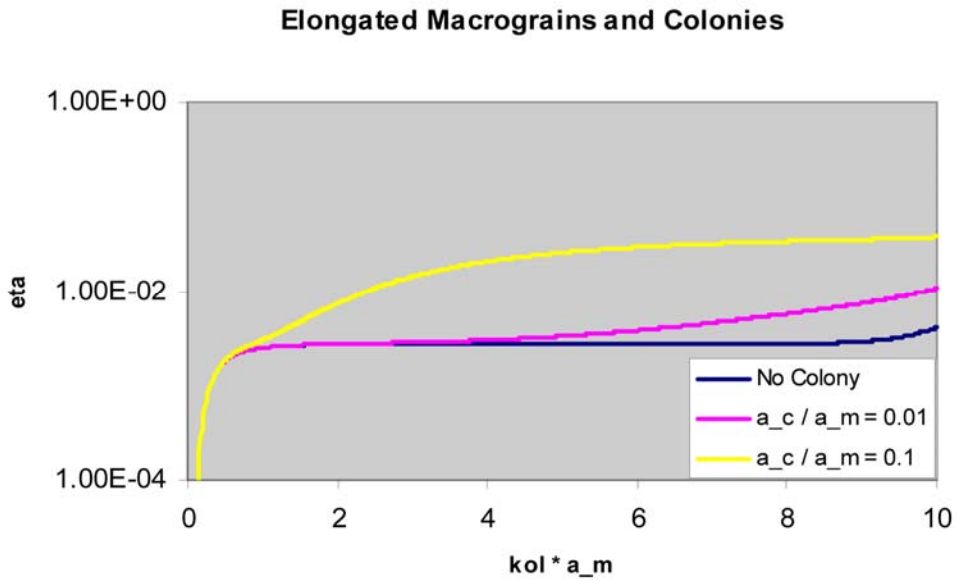

Figure 1.3. Normalized and Absolute Backscatter Coefficients for Ultrasonic Wave Propagating in the 3-Direction of the Sample Coordinate System for Spheroidal Macrograins and Colonies

The implication of the Born approximation utilized in Eq. (1.4) is that multiple scattering events are ignored in the calculation of backscatter power. The formulation of backscatter power given by Eq. (1.9) would include some degree of multiple scattering if δc_{ijkl} would be taken as the fluctuation of local elastic constants measured relative to complex effective elastic constants constructed from wave propagation theory that includes multiple scattering. For example, one can define $\delta c_{ijkl} = c_{ijkl}(\vec{r}) - c_{ijkl}^{eff}$ where c_{ijkl}^{eff} is calculated from the unified theory of Stanke and Kino (1984).

2.0 Theory of Ultrasonic Scattering Attenuation in Single-Phase and Duplex Microstructures

2.1 Mean Wave Propagation

The displacement field due to an ultrasonic wave propagating in a polycrystalline material can be described by the stochastic wave equation Equation Section 2

$$[c^{\xi}_{ijkl}(\vec{r})u^{\xi}_{kl}(\vec{r})]_{,j} + \rho^{\xi}(\vec{r})\omega^2 u^{\xi}_{i}(\vec{r}) = 0\,, \tag{2.1}$$

where $c^{\xi}_{ijkl}(\vec{r})$ is the actual local elastic tensor, $\rho^{\xi}(\vec{r})$ is the actual local density, and $u^{\xi}_{i}(\vec{r})$ is the actual displacement field in the medium ξ. The set of elastic tensors and the probability density function $p(\xi)$, which is the probability of choosing any particular medium, form a stochastic process. In a medium with no density variation, the application of the unified theory of Stanke and Kino (1984) to the wave equation yields the general formula following Christoffel's equation for the expected propagation constant k (Ahmed and Thompson 1996).

$$[\Gamma_{ik} - \rho\omega^2 / k^2\delta_{ik}] = \vec{0} \tag{2.2}$$

where

$$\Gamma_{ik} = \hat{k}_j\hat{k}_l\{c^{o}{}_{ijkl} + \varepsilon < \delta c_{ijkl} > + \varepsilon^2 \int G_{\alpha\gamma}(\vec{s})[\begin{pmatrix} < \delta c_{ij\alpha\beta}(\vec{p}+\vec{s}/2)\delta c_{ij\alpha\beta}(\vec{p}-\vec{s}/2) > - \\ < \delta c_{ij\alpha\beta}(\vec{p}+\vec{s}/2) >< \delta c_{ij\alpha\beta}(\vec{p}-\vec{s}/2) > \end{pmatrix} e^{ik\vec{s}.\hat{k}}]_{,\beta\delta} d^3\vec{s}\},$$

$\varepsilon\delta c_{ijkl} = c_{ijkl}(\vec{r}) - c^{o}{}_{ijkl}$, $G_{\alpha\gamma}(\vec{s})$ is a Green's function taken from the work of Lifshits and Parkhamovski (1950), $c^{o}{}_{ijkl}$ are the Voigt (1928) averaged elastic constants, and $W(\vec{s})$ represents the geometric autocorrelation function (the probability that two points, placed randomly in the material and separated by a displacement $\vec{s}$, fall in the same crystallite). As mentioned earlier, the expected values are denoted by the symbol pair <>. This equation describes the expected propagation constant k of plane waves of the form $< u_i >= a\hat{u}e^{-ik\hat{k}.\vec{r}-i\omega t}$, where ω is the angular frequency and $\vec{k} = k\hat{k}$ is the propagation vector in the direction of propagation $\hat{k}$. k is related to phase velocity v_p and attenuation coefficient α through the relationship $k = \omega / v_p - i\alpha$.

Equation 2.7 allows solutions for $\hat{u}$ only if the determinant of the matrix in brackets on the left-hand side vanishes. In the absence of scattering, these occur for three distinct real values of ω^2 / k^2; one for each of the two quasi-shear waves and one for the quasi-longitudinal wave. In the presence of scattering, requiring the determinant to vanish defines a transcendental equation which may support many roots. The correct root was selected by seeking the real part of the root closest to the root in the absence of

scattering and requiring that the imaginary part $\alpha \geq 0$. The wave polarizations are given by the corresponding eigenvectors.

2.2 Particular Cases for Calculations

In this report, we only consider polycrystals that are statistically homogeneous; that is, the ensemble averages are independent of position. For such media, the two-point averages appearing in Eq. 2.7 can be taken outside the integration sign. First, we present our results for two simple microstructures; one without and the other with macroscopic texture. We then present results for an example duplex microstructure having macrograins and colonies.

2.3 Single-Phase Microstructure

2.3.1 Randomly Oriented Grains:

We first present our calculations for expected propagation constants in polycrystalline materials without macroscopic texture. The generalized Christoffel equation in this becomes

$$\begin{aligned} &[\Gamma_{ik} - \rho\omega^2 / k^2 \delta_{ik}] = \vec{0} \\ &\Gamma_{ik} = \hat{k}_j \hat{k}_l \{c^o{}_{ijkl} + \varepsilon^2 [< \delta c_{ij\alpha\beta} \delta c_{\gamma\delta kl} >] \int G_{\alpha\gamma}(\vec{s}) [P(\vec{s}) e^{ik\vec{s}.\hat{k}}]_{,\beta\delta} d^3\vec{s}\} \end{aligned} . \tag{2.3}$$

$P(\vec{s})$ represents the geometric autocorrelation function (the probability that two points, placed randomly in the material and separated by a displacement $\vec{s}$, fall in the same grain). If $f = f(\varphi, \theta, \psi)$, where (φ, θ, ψ) are the Euler angles, the ensemble average for all random values of Euler angles is given by

$$\langle f \rangle = \frac{1}{8\pi^2} \int_0^{2\pi} \int_0^{\pi} \int_0^{2\pi} f(\varphi, \theta, \psi) \sin\theta \, d\varphi \, d\theta \, d\psi \, . \tag{2.4}$$

2.3.2 [001] Aligned Polycrystals

For simple microstructure with macroscopic texture, the generalized Christoffel equation in this becomes

$$\begin{aligned} &[\Gamma_{ik} - \rho\omega^2 / k^2 \delta_{ik}] = \vec{0} \\ &\Gamma_{ik} = \hat{k}_j \hat{k}_l \{c^o{}_{ijkl} + \varepsilon < \Delta_{ijkl} > + \varepsilon^2 [< \delta c_{ij\alpha\beta} \delta c_{\gamma\delta kl} > - < \delta c_{ij\alpha\beta} >< \delta c_{\gamma\delta kl} >] \int G_{\alpha\gamma}(\vec{s}) [P(\vec{s}) e^{ik\vec{s}.\hat{k}}]_{,\beta\delta} d^3\vec{s}\} \end{aligned} . \tag{2.5}$$

The particular texture considered here is where the [001] crystallographic axes of all grains parallel to the *z*-axis of the laboratory coordinate system while the [100] and the [010] axes are randomly oriented about this direction. This simplifies the averaging procedure. Thus, if φ is the rotation of the [100] axis from the *x*-axis in the laboratory system,

$$< f >= \frac{1}{2\pi} \int_0^{2\pi} f(\varphi) d\varphi \tag{2.6}$$

Following the general procedure to obtain the complex propagation constants and polarizations as described before, we were able to develop an integral equation for the expected propagation constant for elastic waves propagating along arbitrary directions in the *yz*-plane. In order to do this, it was found convenient to rotate the laboratory coordinate system (*x, y, z*) by an angle θ about the *x*-axis resulting in a primed (*x′=x, y′, z′*) coordinate system and choose the z' -axis (direction 3) as the propagation direction. Waves with arbitrary propagation direction are, in general, not purely longitudinal or shear in a medium with macroscopic texture. However, for cubic crystals with small single crystal anisotropy $A = c_{11} - c_{12} - 2c_{44}$ compared to $c^o{}_{ijkl}$, the deviations of the polarizations from those of pure modes are not expected to be large. Therefore, we have neglected the deviation of the polarizations from the pure mode values in the polycrystalline aggregate under consideration. With this assumption, we only need the averages $\varepsilon < \delta c_{3333} >$ and $\varepsilon^2[< \delta c_{33kl}\delta c_{mn33} > - < \delta c_{33kl} >< \delta c_{mn33} >]$.

2.3.3 Duplex Microstructure

For duplex microstructures composed of randomly oriented macrograins, using the notations employed earlier in the discussions of backscatter, the Christoffel equation can be written as

$$\begin{aligned} &[\Gamma_{ik} - \rho\omega^2 / k^2 \delta_{ik}] = \vec{0} \\ &\Gamma_{ik} = \hat{k}_j \hat{k}_l \{c^o{}_{ijkl} + D^M_{ijkl\alpha\beta\gamma\delta} \int G_{\alpha\gamma}(\vec{s})[P^M(\vec{s}) e^{ik\vec{s}.\hat{k}}]_{,\beta\delta} d^3\vec{s}\} + D^C_{ijkl\alpha\beta\gamma\delta} \int G_{\alpha\gamma}(\vec{s})[P^C(\vec{s}) e^{ik\vec{s}.\hat{k}}]_{,\beta\delta} d^3\vec{s}\} \end{aligned} . \tag{2.7}$$

Here

$$\begin{aligned} D^M_{ijkl\alpha\beta\gamma\delta} &= \frac{\varepsilon^2}{N_{distinct}} \left[\left\langle \delta c^P_{ijkl} \delta c^P_{\alpha\beta\gamma\delta} \right\rangle + \sum_{P \neq Q} \left\langle \delta c^P_{ijkl} \delta c^Q_{\alpha\beta\gamma\delta} \right\rangle \right] \text{ and} \\ D^C_{ijkl\alpha\beta\gamma\delta} &= \frac{\varepsilon^2}{N_{distinct}} \left[(N_{distinct} - 1) \left\langle \delta c^P_{ijkl} \delta c^P_{\alpha\beta\gamma\delta} \right\rangle - \sum_{P \neq Q} \left\langle \delta c^P_{ijkl} \delta c^Q_{\alpha\beta\gamma\delta} \right\rangle \right] \end{aligned} \tag{2.8}$$

2.4 Results and Discussions: Expected Wave Propagation Constants

We present numerical results for three different idealized polycrystalline aggregates: (1) equiaxed/ elongated grains with random crystallographic orientation, (2) equiaxed/elongated grains with preferential [001] alignment, and (3) randomly oriented equiaxed/elongated macrograins encountered in duplex stainless steel. In presenting our results, we have used $h = 2c$ (macrograin/colony longer dimension) and $d = 2a$ (transverse diameter). The schematic diagram of an ellipsoidal grain was shown in Figure 1.1. In all our calculations, the crystallites are considered to possess cubic symmetry. Table 1.1 lists single crystal elastic constants and density of the polycrystals (Kupperman and Reimann 1978).

2.4.1 Randomly Oriented Grains

The frequency dependence of the normalized attenuation coefficient (attenuation per wavelength) of plane longitudinal waves in steel with randomly oriented grains is shown in Figure 2.1. The direction of the plane ultrasonic wave makes 45° with respect to the *z*-axis of the laboratory coordinate system. The major axis of the ellipsoidal grain coincides with the *z*-axis. The grain aspect ratio d / h = 1 corresponds to equiaxed grains. For a fixed value of $k_{ol}d$, we see that grain elongation (indicated by d / h < 1) causes larger attenuation in all the frequency regimes (Rayleigh, stochastic, and geometric). The transitions between these regimes are also clearly affected by increasing grain elongation. Figure 2.2 shows the phase velocity dispersion over a wide frequency range. At low frequencies, the phase velocity of the mean longitudinal wave is predicted to be smaller than that obtained by the unweighted Voigt averaged elastic constant of a polycrystal. However, at higher frequencies, the unified theory of Stanke and Kino (1984) over predicts phase velocities. The grain shape is also seen to affect the expected phase velocity. Figure 2.3 and Figure 2.4, showing absolute attenuation coefficient and phase velocity, are constructed from the results shown in Figure 2.1 and Figure 2.2 by choosing average grain diameter d.

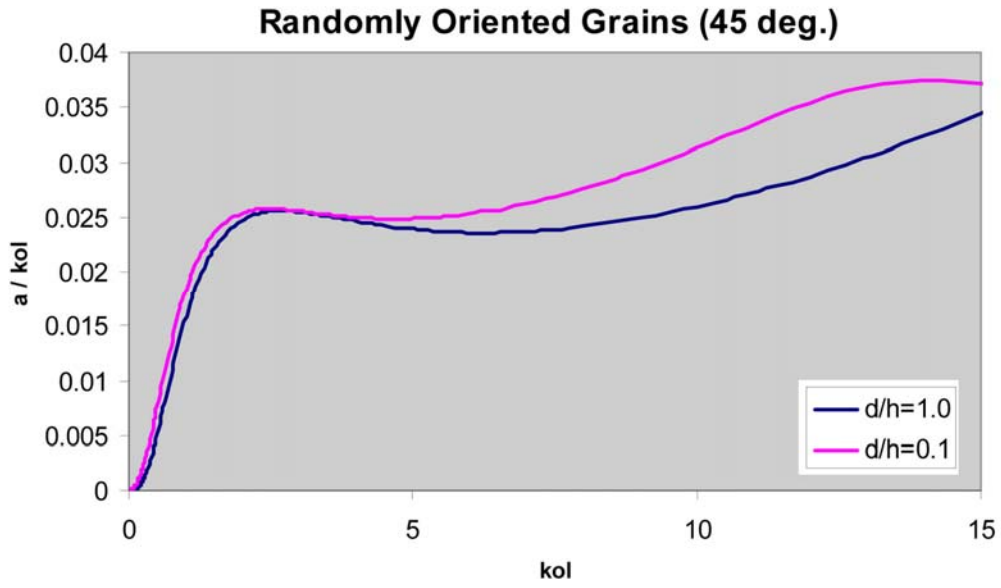

Figure 2.1. Frequency Dependence of Normalized Attenuation Coefficient of Plane Longitudinal Waves in Steel with Randomly Oriented Grains (propagation direction makes 45° with respect to the *z*-axis)

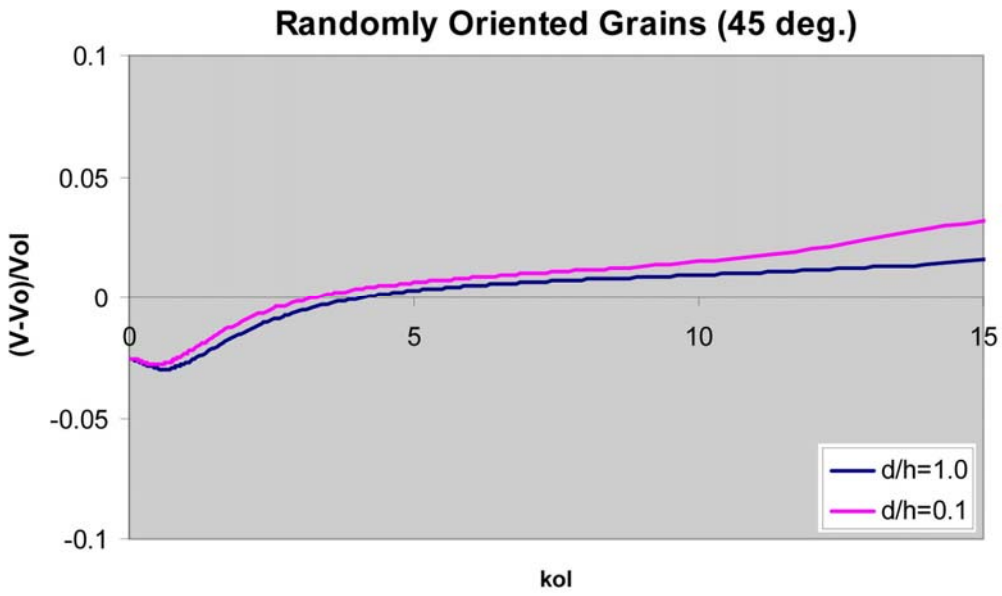

Figure 2.2. Frequency Dependence of Normalized Phase Velocity of Plane Longitudinal Waves in Steel with Randomly Oriented Grains (propagation direction makes 45° with respect to the *z*-axis)

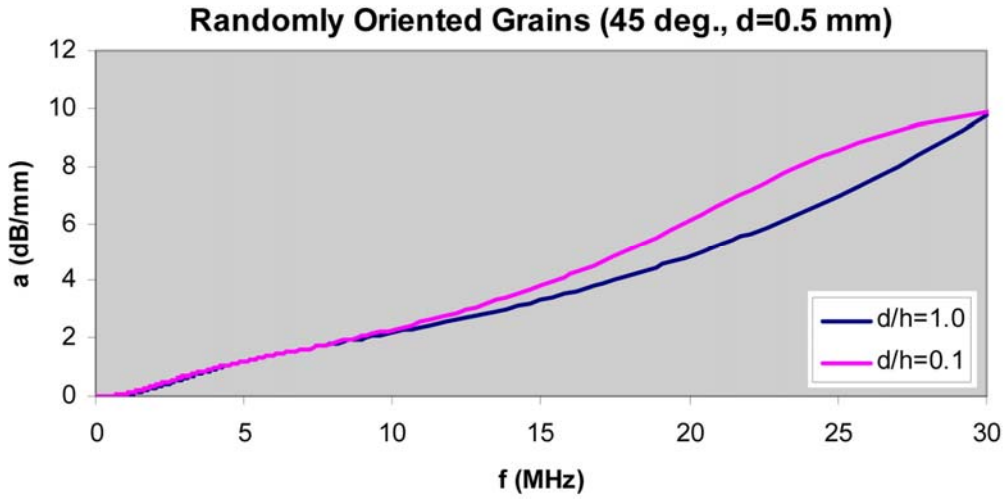

Figure 2.3. Frequency Dependence of Attenuation Coefficient of Plane Longitudinal Waves in Steel with Randomly Oriented Grains (propagation direction makes 45° with respect to the *z*-axis)

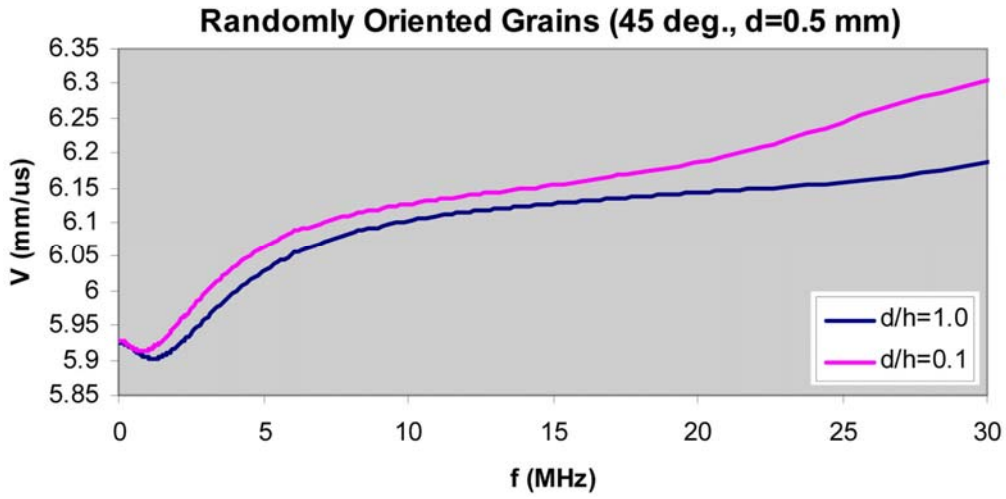

Figure 2.4. Frequency Dependence of Phase Velocity of Plane Longitudinal Waves in Steel with Randomly Oriented Grains (propagation direction makes 45° with respect to the *z*-axis)

2.4.2 [001] Aligned Stainless Steel

In Figure 2.5, we describe the frequency dependence of the normalized attenuation coefficient of plane longitudinal waves propagating in steel with perfectly aligned [001] crystallographic axes; the wave vector making 45° with the *z*-axis. Both the major axis of the ellipsoidal grain and [001] the crystallographic axis coincide with the *z*-axis in this case. Similar to the case observed for randomly oriented grains, larger grain elongation (indicated by smaller d/h ratio) causes a somewhat larger attenuation for a given non-dimensional frequency. Phase velocity dispersion is described next in Figure 2.6. The phase velocity predicted by the unweighted Voigt averaged elastic constant is seen to under predict at all frequencies shown. Figure 2.7 and Figure 2.8 show the absolute attenuation coefficient and phase velocity when the mean transverse grain diameter is 500 μm. Figures 2.9–2.12 describe the case when the mean ultrasonic wave makes 90° with the *z*-axis. The difference in magnitudes between these cases is the result of two factors: the difference in two-point elastic constant correlation and the difference in the mean path crossed by the ultrasonic wave across a grain.

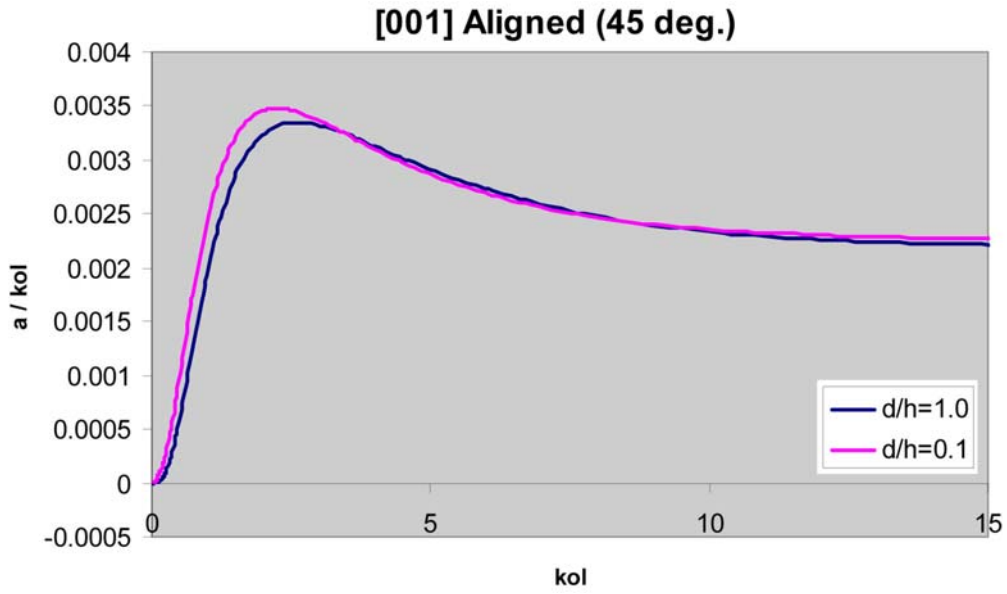

Figure 2.5. Frequency Dependence of Normalized Attenuation Coefficient (attenuation per wavelength) of Plane Longitudinal Waves in Steel with [001] Aligned Grains (propagation direction makes 45° with respect to the *z*-axis)

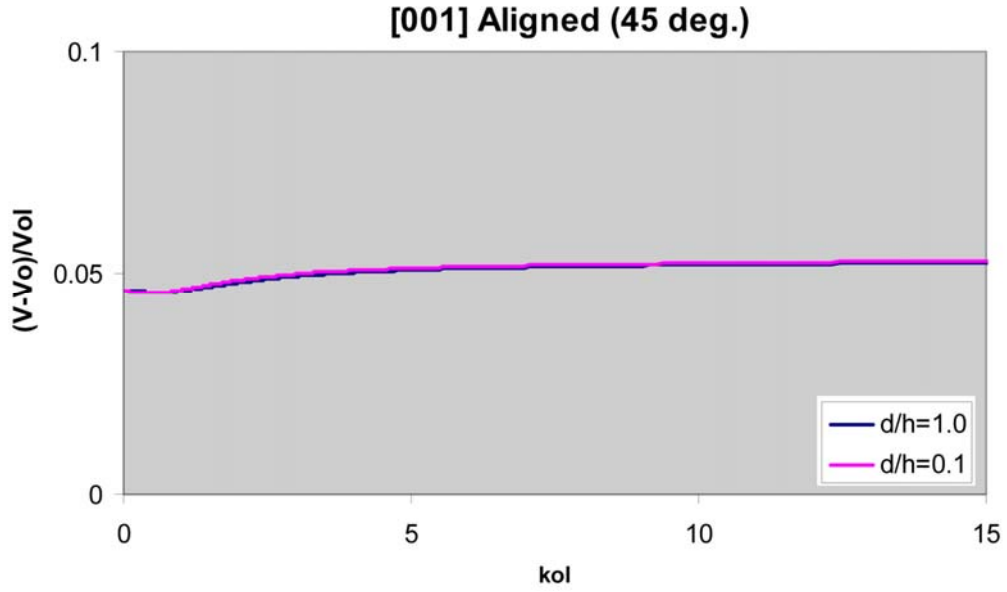

Figure 2.6. Frequency Dependence of Normalized Phase Velocity of Plane Longitudinal Waves in Steel with [001] Aligned Grains (propagation direction makes 45° with respect to the *z*-axis)

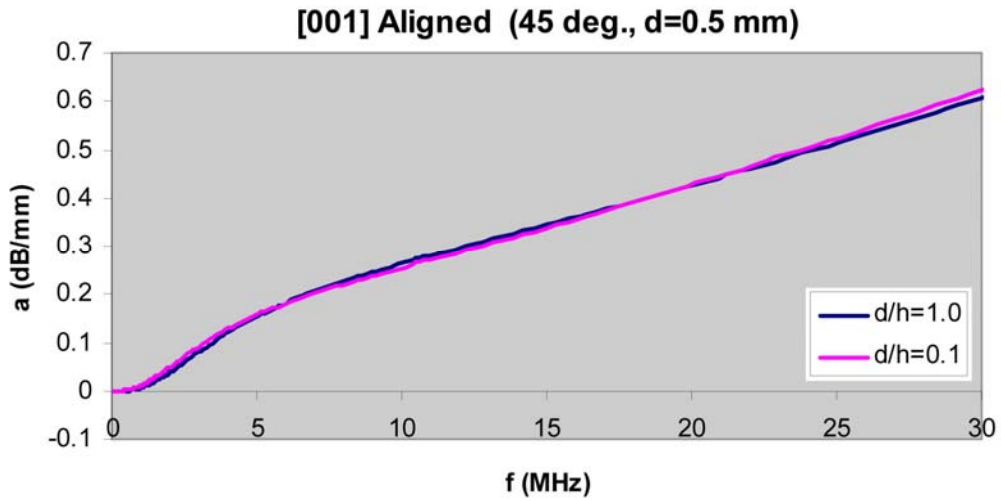

Figure 2.7. Frequency Dependence of Attenuation Coefficient of Plane Longitudinal Waves in Steel with [001] Aligned Grains (propagation direction makes 45° with respect to the *z*-axis)

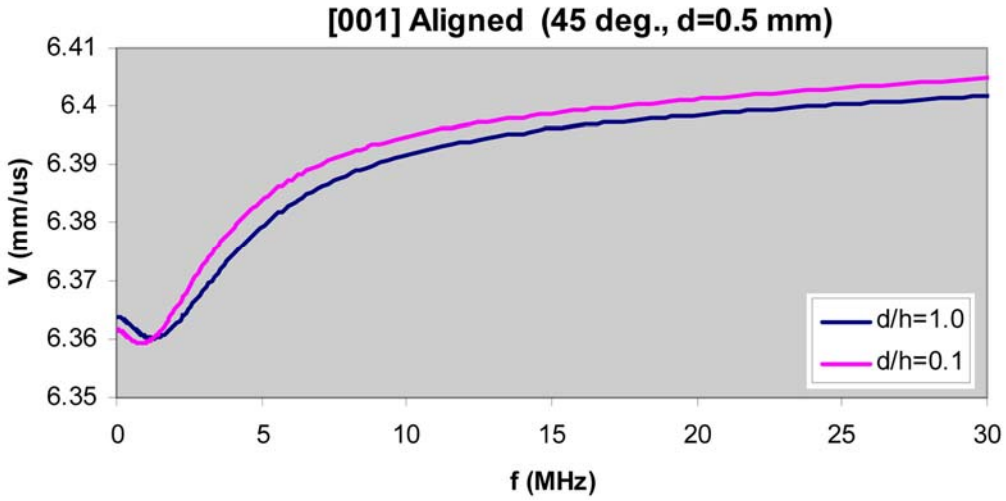

Figure 2.8. Frequency Dependence of Phase Velocity of Plane Longitudinal Waves in Steel with [001] Aligned Grains (propagation direction makes 45° with respect to the *z*-axis)

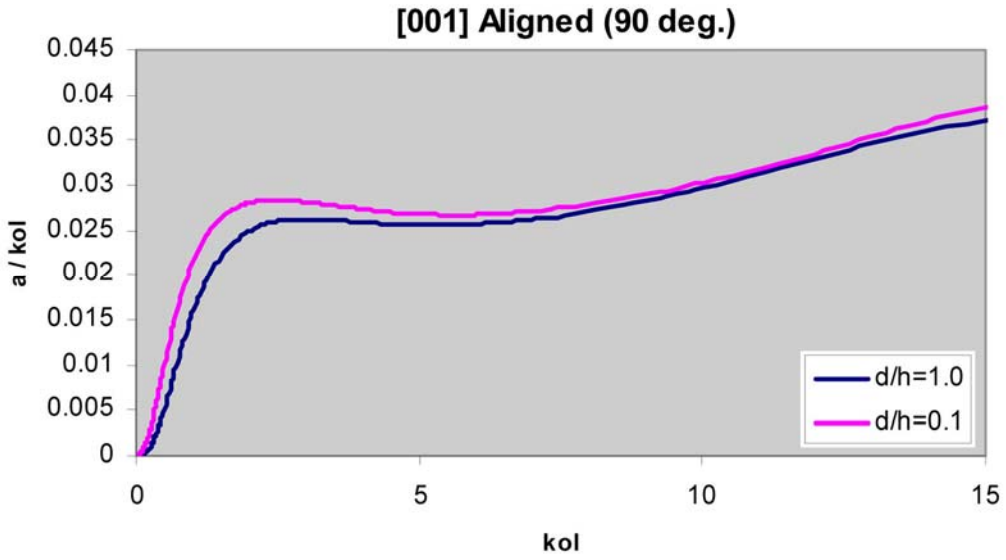

Figure 2.9. Frequency Dependence of Normalized Attenuation Coefficient (attenuation per wavelength) of Plane Longitudinal Waves in Steel with [001] Aligned Grains (propagation direction makes 90° with respect to the *z*-axis)

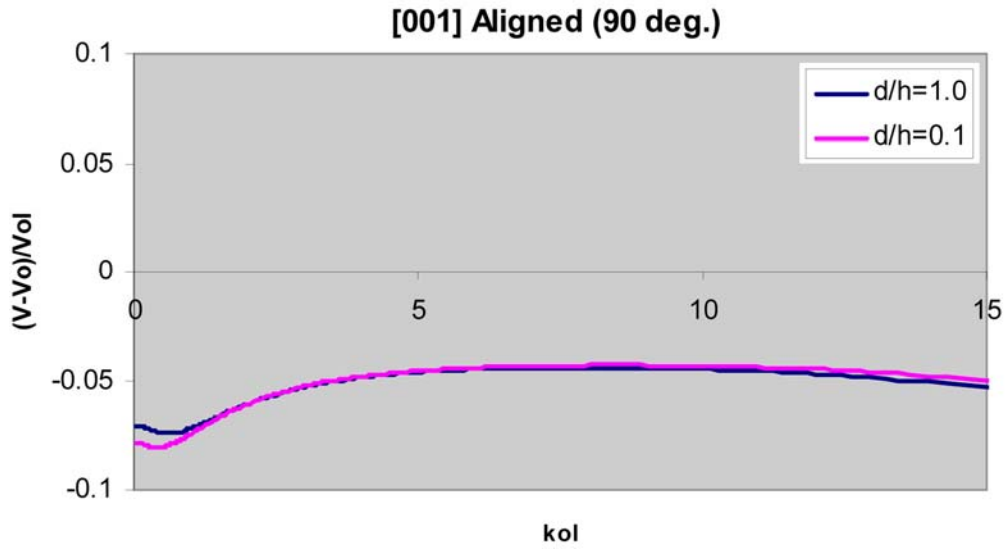

Figure 2.10. Frequency Dependence of Normalized Phase Velocity of Plane Longitudinal Waves in Steel with [001] Aligned Grains (propagation direction makes 90° with respect to the *z*-axis)

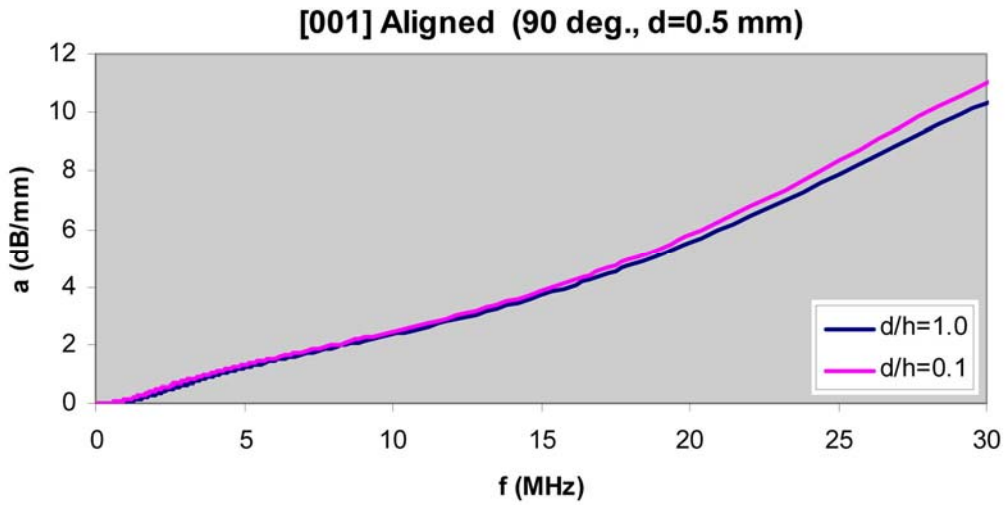

Figure 2.11. Frequency Dependence of Attenuation Coefficient of Plane Longitudinal Waves in Steel with [001] Aligned Grains (propagation direction makes 90° with respect to the *z*-axis)

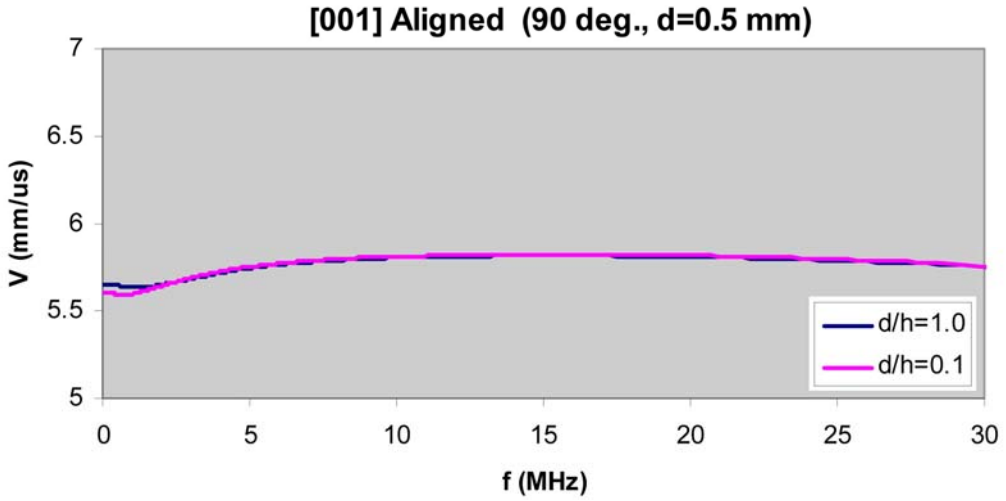

Figure 2.12. Frequency Dependence of Attenuation Coefficient of Plane Longitudinal Waves in Steel with [001] Aligned Grains (propagation direction makes 90° with respect to the *z*-axis)

2.5 Duplex Microstructure

2.5.1 Duplex Steel

We next present theoretical predictions of the expected attenuation coefficient and phase velocity of ultrasonic waves propagating in our realization of the duplex steel. In our calculations, we have assumed the macrograins to have random orientation. First, we assume the macrograins and colonies to be equiaxed; the relative sizes of the colonies are allowed to vary. As one would expect, Figure 2.13 shows that as the colony size increases, the attenuation due to scattering also increases. When the colony sizes

are smaller than 1% of that of a macrograin, their contribution to attenuation is negligible. Noticeable amplification in attenuation is observed when the ratio of colony diameter to macrograin diameter is 0.1 at frequencies corresponding to normalized frequencies $k_{ol}d > 2$. Phase velocity dispersion is shown next in Figure 2.14. The colony size is seen to have a negligible effect on phase velocity. Figure 2.15 and Figure 2.16 illustrate the effect of macrograin/colony shape on attenuation and velocity dispersion, respectively. In this case, however, the additional contribution of colonies due to their sizes becomes noticeable for normalized frequencies $k_{ol}d \geq 1$.

Comparing results for duplex steel with those of the single-phase randomly oriented grains, it is seen that the attenuation is considerably higher in duplex steel. In addition, if the colonies themselves are of sizes comparable to their parent macrograin, their contribution to the scattered field become more pronounced.

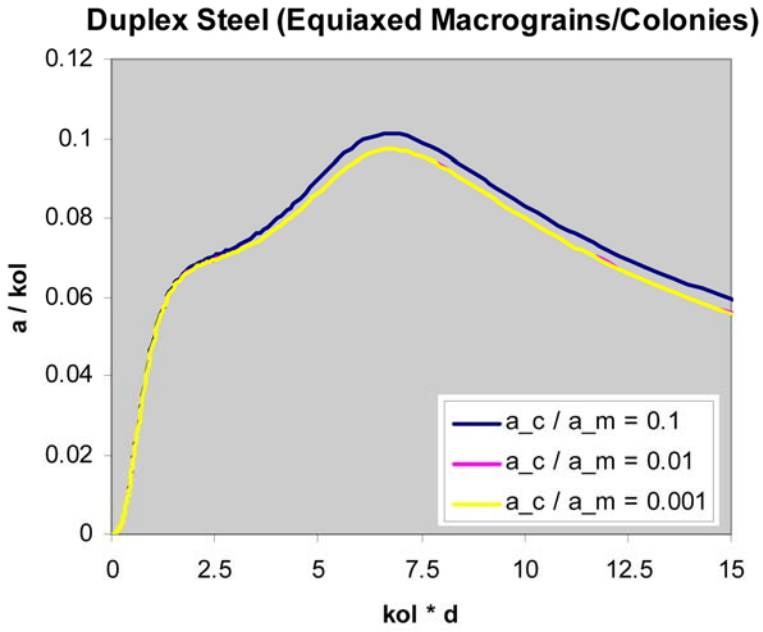

Figure 2.13. Frequency Dependence of Normalized Attenuation Coefficient of Plane Longitudinal Waves in Duplex Steel with Randomly Oriented Equiaxed Macrograins and Colonies (propagation direction makes 45° with respect to the z-axis)

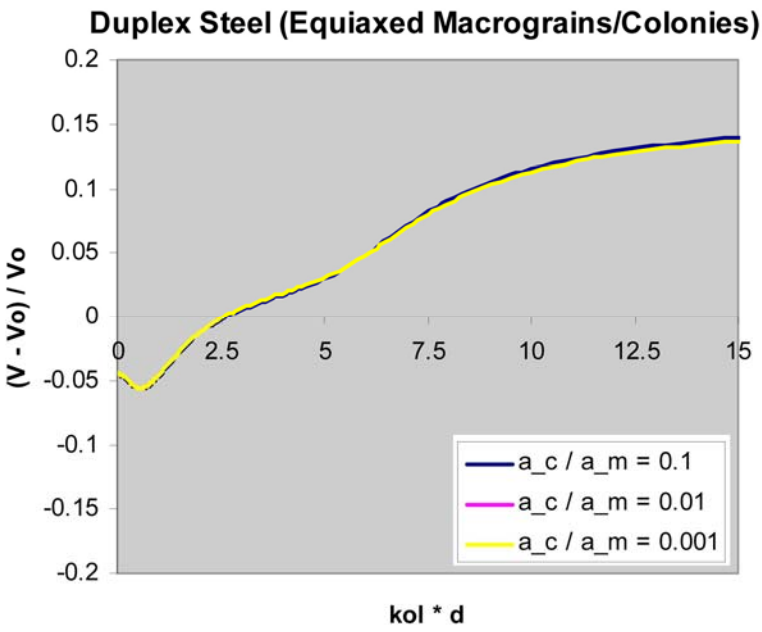

Figure 2.14. Frequency Dependence of Normalized Phase Velocity of Plane Longitudinal Waves in Duplex Steel with Randomly Oriented Equiaxed Macrograins and Colonies (propagation direction makes 45° with respect to the *z*-axis)

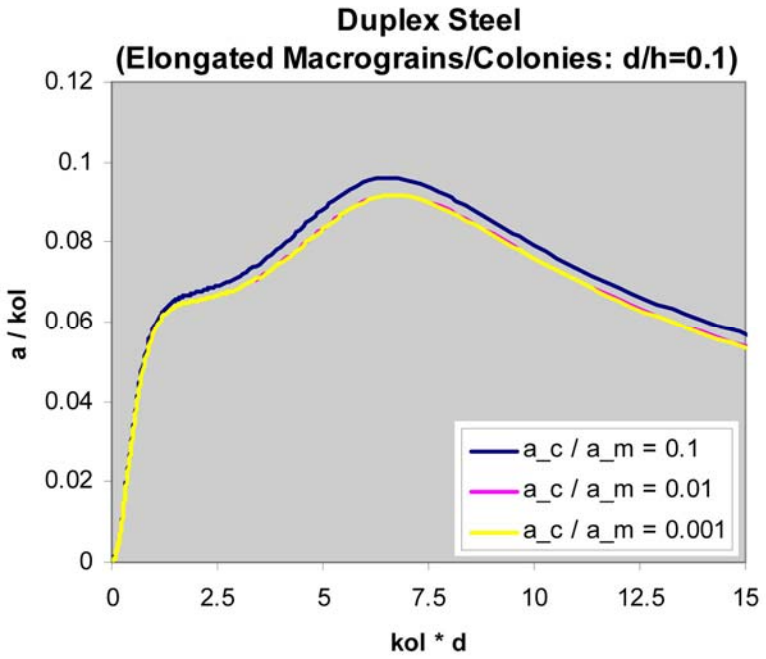

Figure 2.15. Frequency Dependence of Normalized Attenuation Coefficient (attenuation per wavelength) of Plane Longitudinal Waves in Duplex Steel with Randomly Oriented Elongated Macrograins and Colonies (propagation direction makes 45° with respect to the *z*-axis)

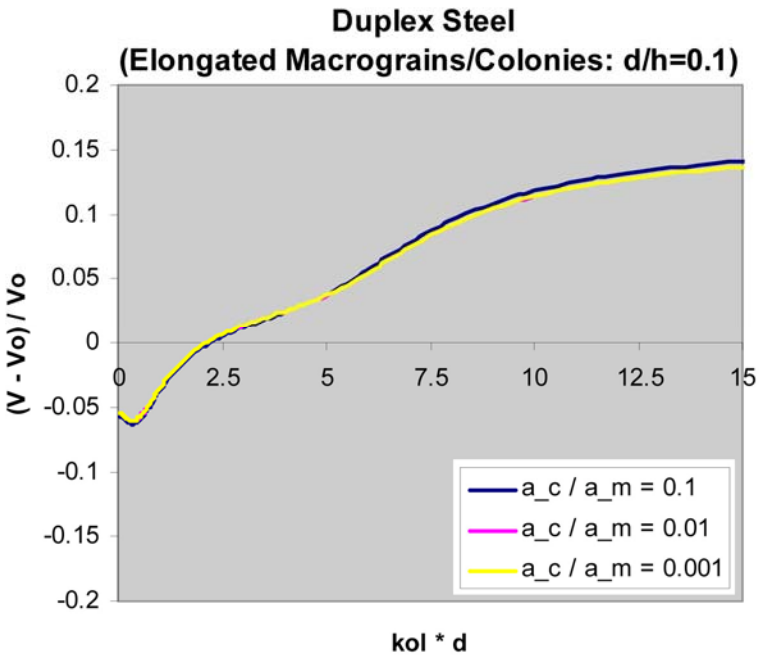

Figure 2.16. Frequency Dependence of Normalized Phase Velocity of Plane Longitudinal Waves in Duplex Steel with Randomly Oriented Elongated Macrograins and Colonies (propagation direction makes 45° with respect to the *z*-axis)

3.0 Conclusions

Numerical predictions presented here suggest that backscatter is dominated by scattering from macrograin boundaries for low non-dimensional frequencies, ka_m. Colonies do not cause noticeable additional backscatter for $ka_m \leq 2$ in the case of equiaxed macrograins and colonies. This threshold frequency at which contributions from colonies are visible is reduced ($ka_m \approx 1$) for elongated macrograins and colonies. Attenuation of plane longitudinal waves in duplex steel with randomly oriented macrograins is seen to be considerably higher than that in single-phase polycrystals with randomly oriented grains. The effect of colony size on attenuation follows the same pattern as that of backscatter power.

4.0 References

Ahmed S and RB Thompson. 1991. "Effect of Preferred Grain Orientation and Grain Elongation on Ultrasonic Wave Propagation in Stainless Steel." In *Review of Progress in Quantitative Nondestructive Evaluation. Vol. 11B; Proceedings of the 18th Annual Review*, pp. 1999-2006. July 28-August 2, 1991, Brunswick, Maine.

Ahmed S and RB Thompson. 1996. "Propagation of Elastic Waves in Equiaxed Stainless-Steel Polycrystals with Aligned [001] Axes." *Journal of Acoustical Society of America* **99**:2086-2096.

Han YK and RB Thompson. 1997. "Ultrasonic Backscattering in Duplex Microstructures: Theory and Application to Titanium Alloys." *Metallurgical and Materials Transactions A* **28A**(1):94-104.

Kupperman DS and KJ Reimann. 1978. "Effect of Shear-Wave Polarization on defect detection in Stainless Steel Weld Metal." *Ultrasonics* **16**(1):21-27.

Kurdjumov G and G Sachs. 1930. "Uber den Mechanismus tier Stahlhartung." *Z. Phys.* **64**:325-343.

Lifshits IM and GD Parkhamovski. 1950. "Theory of Propagation of Supersonic Waves in Polycrystals." *Zhur. Eksptl. Teoret. Fiz.* **20**:175-182.

Rose JH. 1992. "Ultrasonic Backscatter from Microstructure." In *Review of Progress in Quantitative Nondestructive Evaluation (QNDE), Vol. 11*, pp. 1677-1684. eds: DO Thompson and DE Chimenti. Plenum Press, New York.

Stanke FE and GS Kino. 1984. "A Unified Theory for Elastic Wave Propagation in Polycrystalline Materials." *Journal of Acoustical Society of America* **75**:665-681.

Thompson RB and TA Gray. 1993. "A Model Relating Ultrasonic Scattering Measurements through Liquid-solid Interfaces to Unbounded Medium Scattering Amplitudes." *Journal of Acoustical Society of America* **74**(4):1279-1290.

Voigt W. 1928. *Lehrbuch der Kristallphysik*. B.G. Teubner, Leipzig, Berlin.

Pacific Northwest
NATIONAL LABORATORY

U.S. DEPARTMENT OF
ENERGY

902 Battelle Boulevard
P.O. Box 999
Richland, WA 99352
1-888-375-PNNL (7665)
www.pnl.gov